

Received: 2014.05.28
Accepted: 2014.07.01
Published: 2014.11.23

Efficacy of Combined Therapy of Periosteum and Bone Allograft in a Critical-Sized Defect Model in New Zealand White Rabbits

Authors' Contribution:
Study Design A
Data Collection B
Statistical Analysis C
Data Interpretation D
Manuscript Preparation E
Literature Search F
Funds Collection G

A **Dawei Zhang**
AG **Dong Huang**
B **Yongjun Huang**
B **Yuanhang Liu**
C **Bochuan Lin**
C **Chaoqun Yu**
D **Yong Mou**
E **Weichi Wu**
F **Huiru Zhang**
F **Hao Lin**

Department of Traumatic and Microsurgical, The Third Affiliated Hospital of Southern Medical University and Second People's Hospital of Guangdong Province, Guangzhou, China

Corresponding Author: Dong Huang, e-mail: huangdong177@126.com

Source of support: This experiment is supported by Guangdong Natural Science Foundation (S2011010001347)

Background: Large segmental bone defects caused by trauma, infection, or bone tumor resection are difficult to cure and have been a problem in the field of bone repair for decades. The objective of this study was to discuss the efficacy of combined therapy of free periosteum and bone allograft in treating bone defects and to provide a theoretical basis for clinical application of this therapy.

Material/Methods: A unilateral tibia cortical defect model in New Zealand white rabbits was established according to Girolamo method. Total 48 rabbits were randomized into 3 groups: a simple bone defect group (n=16), an autogenous bone graft group (n=16), and a periosteum and bone allograft combined therapy group (n=16). The efficacy was evaluated by imaging inspections and scoring, HE staining, and RT-PCR in postoperative weeks 2, 4, 8, and 12.

Results: The results of imaging and histopathological inspections in the study indicated that in postoperative weeks 4, 8, and 12 the experimental and control groups had statistically significant differences in Lane-Sandhu radiographic scoring and relative bone density when compared with the simple bone defect group (P<0.05). The RT-PCR results suggested that the expression of SPP-1, BMP-2, and VEGF in the experimental group was higher than in the control group (P<0.05) and the expression of Col 1 α 1 in the control group was higher than in the experimental group (P<0.05).

Conclusions: Efficacies of the combined therapy (periosteum combined with bone allografting) and the criterion standard therapy (autogenous bone grafting) are equivalent in treating bone defects in New Zealand white rabbits.

MeSH Keywords: **Bone Diseases • Bone Transplantation • Periosteum • Rabbits**

Full-text PDF: <http://www.medscimonit.com/abstract/index/idArt/891103>

 3825

 4

 5

 28



Background

Large, segmental bone defects caused by trauma, infection, or bone tumor resection are difficult to cure and have been a problem in the field of bone repair for decades. At present, available therapies include periosteum graft repairing, bone autograft and allograft transplantation, artificial material filling, bone lengthening technology, and tissue engineering technology [1–3]. These methods are efficacious to some extent in treating bone defects, but all have some deficiencies, including rapid bone degradation, bone allograft resorption, bone nonunion, and the risk of refracture. Autogenous bone grafts, the criterion standard for bone defect treatments, have many advantages, including fewer postoperative complications and high osteogenic capability. Zouboset et al. [4] used modified Matti-Russe technique with autogenous bone transplantation for treatment of scaphoid non-union and pseudarthrosis and achieved satisfactory results. Xue Tao Xie et al. [5] succeed in using free vascularized fibular graft in combination with a locking plate on a 47-year-old female patient. These reports all suggest that autogenous bone graft transplantation could efficiently cure bone defect. Because material resources are limited, autogenous bone grafts are not applicable where there are large amounts of bone defects. Therefore, it is important to find a therapy that can fill bone defects effectively with stents made of convenient materials as well as promoting rapid bone formation. Maculéet et al. [6] used combined therapy of fascia lata and allograft in treating large-scale bone loss after total knee arthroplasty, which achieved satisfactory results. This methods offer us a new way of thinking about treatment of bone defects. Based on both the creeping substitution theory and bone induction theory, the combined therapy of vascularized periosteum and bone allograft became the best method for treating bone defects caused by a variety of reasons [7].

Periosteum can be divided into 2 layers – the outer one is the fibrous layer and the inner one is the germinal layer. The fibrous layer prevents non-osteogenic cells from growing into a bone defect. The germinal layer has a small amount of fibrous material and is rich in vessels and cells, including osteoprogenitor cells, osteoblasts, osteoclasts, and vascular endothelial cells. It has a high osteogenic capability, so it also is called the osteogenic layer [8–11]. Using histomorphology and ultrastructure CT examinations, several researchers have found that removing periosteum from living autogenous bone leads to a 73% decrease in new bone and cartilage, a 10-fold decrease in new vessels, and a 75% decrease in osteoclasts [12]. Poussa et al. [13] examined microangiographic technology and found that capillaries formed, without a blood supply, in the first day after free periosteum grafting. Capillaries can enter directly into the germinal layer of the free periosteum through the surrounding soft tissues and support the osteogenesis. Berggren et al. [14] evaluated bone grafting and periosteum grafting by using scintigraphic scans and found that

osteogenesis progressed faster in periosteum, suggesting that a free periosteum graft has a great osteogenic capability and is able to repair both bone nonunion and bone defects.

In simple periosteum grafting, however, there is no stent filling the bone defect. Moreover, simple periosteum grafting cannot achieve the therapeutic goal. Filling and osteoconduction in large segmental bone defects are crucial for bone healing. Allograft bone transplantation has developed rapidly since it was first used clinically by MacEwen 1980. The healing process of allograft bone transplantation involves revascularization of bone allograft, formation of new bone, the union of the host's bone bed and the graft, and the fulfillment of bone incorporation. Radiological and histological studies in massive bone allografts, however, confirmed that the repair process of cortical bone allografts was extremely slow. The newly formed bone could only permeate into the necrotic bone by a few millimeters [15]. With such limited osteogenic effect and repair capability, the incidence of bone allograft nonunion and early-stage fracture incidence reached 20% [16]. In our study design, bone allografts, wrapped with periosteum, were able to repair bone defects. The osteoconduction and stent effect of bone allografts can support the creeping substitution repair process. In addition, the periosteum itself has capabilities of early osteogenesis and osteoinduction, promoting the bone healing process.

The aim of this study was to discuss the possible repair mechanism of the combined therapy of free periosteum and bone allografts in treating bone defects and to provide the theoretical basis for the clinical application of this therapy.

Material and Methods

Experimental animals

A total of 48 New Zealand white rabbits, each weighing 2–3 Kg, were kept for 1 week prior to the study with the same feed and under the same living conditions. There were 3 groups with 16 rabbits each – a blank group, an autogenous bone transplant group (control group), and a group with allografts with bone membrane transplants (experimental group).

Bone allograft harvest

Allograft bone was harvested from limbs of New Zealand white rabbits (mature and of either sex), trimmed to segments 2–2.5cm long, and used in the subperiosteal implantation.

Grafts were stripped of soft tissue, cleaned with detergent, hydrogen peroxide, and ethanol sonication washes, and then allowed to dry fully [17]. Samples were irradiated by Cobalt-60 (25 kGy) for sterilization, and then stored at –20°C until used.

Table 1. Lane-Sandhu radiographic scoring system.

Degree of bone formation	No new bone formed	0
	The area of new bone accounts for 25% of the defect area	1
	The area of new bone accounts for 50% of the defect area	2
	The area of new bone accounts for 75% of the defect area	3
	The area of new bone accounts for 100% of the defect area	4
Degree of union	Fracture line is fully visible	0
	Fracture line is partially visible	2
	Fracture line is not visible	4
Degree of medullary cavity remodeling	No sign of remodeling	0
	Recanalization of medullary cavity	2
	Cortical bone structure forms after recanalization of medullary cavity	4

Subperiosteal implant and bone defect surgeries

All animals, which were obtained from the Southern Medical University (Guangzhou, Guangdong, China) had surgeries that were performed according to an approved protocol created by the Southern Medical University Animal Care and Use Committee. In the subperiosteal implant study, 48 New Zealand white rabbits (mature of either sex) weighing 2–3 Kg were assigned randomly to 3 different experimental groups (n=16): blank group, control group, and experimental group. Anesthesia was induced with 2% sodium pentobarbital by intravenous injection (1 ml/kg IP). Following anesthetization, the skin was sterilized with 0.5% iodophor. A longitudinal incision was made through the skin and periosteum over the surface of the left tibia and over the sagittal suture. For creating the tibia bone defect models, a 15-mm bone defect was created according to the method of Girolamo [18]. For the blank group, no allograft was replaced in the defect; in the control group, autogenous bone was replaced in the defect; and in the experimental group, periosteum was elevated over the defect bones to a diameter of 2 cm before the allograft was replaced. Then, the periosteum was closed with a 5–0 running nylon suture. The skin was closed with a 0–0 running nylon suture. Penicillin was given once a day by intramuscular injection after closure for 3–5 days to prevent infection. Rabbits were given free access to food and water and monitored for complications or abnormalities. At 2, 4, 8, and 12 weeks post-surgery, 12 rabbits were anesthetized with 2% sodium pentobarbital and injected intravenously with a barbiturate (100 mg/kg) for euthanasia.

X-Ray examination

Radiographs were taken at 2, 4, 8, and 12 weeks after the experiments, and points were allotted according to the Lane-Sandhu scoring system [19]. All the points were given by 3 independent examiners who were trained in the Lane-Sandhu

system. The points were given according to the degree of bone formation, connections, and bone marrow recanalization. For bone formation, fully formed was given 4 points and no bone formation was given zero points. For the degree of connection, according to the clearance of fracture line, was given zero, 2, and 4 points. No fracture line detected was given 4 points, and a clear fracture line was given zero points. For bone marrow recanalization, according to the degree of recanalization, zero, 2, or 4 points was given. The Lane-Sandhu radiographic scoring system is explained in Table 1.

Bone density detection (BMD)

Measurement of BMD was conducted using a Hologic QDR-2000/Plus DXA instrument (70 kVp/140 kVp). After carefully separating the tibia at the site of modeling and completely removing the superficial muscles and soft tissues, BMD was expressed in grams per cm².

Histology

Following *in vivo* X-Ray scanning and *ex vivo* bone density detection, 24 tibia samples were fixed in 10% buffered formalin for 7 days and decalcified using an HCl and EDTA decalcifying solution for 3 days at 4°C with agitation. The bone was cut in half and centered at the defect or implant. The sample was stored in 70% ethanol until paraffin embedding for hematoxylin and eosin (H&E) staining.

Fluorescence quantitative PCR detection

Total mRNA was extracted from the 24 tibia samples with the TRizol reagent (Invitrogen, Carlsbad, CA). PrimeScript RT Master Mix (Takara, Japan) was used to synthesize the first strand of complementary DNA. Briefly, 2 µg of total RNA was used to synthesize cDNA. Products were amplified using a SYBR Green

Table 2. List of PCR primers.

PCR	F (5'–3')	R (5'–3')
COL1A1	TTCAGCTTTGTGGACCTCCG	GTTCTGCACGCATGTGACTG
BMP2	GGGTGGAACGACTGGATTGT	TGCACGATGGCATGGTTAGT
SPP1	GCGTGGAACCCAAAGTCAC	CACGGAGTTGTCTGTGCTCT
VEGF	TTCATGGAAGTCTACCGGCG	TGACGTTGAACTCCTCGGTG
GAPDH	CATGAGAAGTATGACAACAGCCT	AGTCCTCCACGATACCAAAGT

PCR Kit (Roche). The amplification condition consisted of incubations at 95°C for 1 min, 60°C for 1 min, and 72°C for 1 min, for a total of 40 cycles. The 7900 HT Real-Time PCR System (Applied Biosystems, Carlsbad, CA) was used to detect real-time PCR. Expression level was normalized against endogenous GAPDHs for related gene expression. Primer sequences for qPCR are listed in Table 2.

Statistical significance

The results are presented as mean \pm standard error of the mean. All statistical analysis was performed by SPSS 13.0 (San Rafael, CA), using the homogeneity test of variance, a one-way General Linear ANOVA, followed by a SNK-t test. Significance was asserted at $p < 0.10$ for homogeneity test of variance, and $p < 0.05$ for one-way General Linear ANOVA and SNK-t test.

Results

Gross examination

After 2 weeks, the defects could be seen clearly, and they were replaced by soft tissue. But at 4, 8, and 12 weeks into the study, the defects were replaced by firm tissue, which provided stability to the defect area in all the groups. The newly formed tissue showed continuity with the surrounding tissues.

Radiological examination

After 2 weeks into the study, the bone density at the bone defect site was low in all 3 groups. A shadow of residual bone allograft was visible in both the control and experimental groups. No obvious bone callus formation was observed any of the 3 groups. At 4 weeks, a few bone calluses formed around the bone defect site, and the density at the bone defect site decreased in the blank group. In the control group and experimental group, the bone density at the bone defect site decreased, but was higher than in the blank group. The bone allograft shadow also was visible. The shadow of the bone allograft, as well as bone callus formation, was more obvious in

the experimental group than in the control group. At 8 weeks, bone callus formation was visible around the bone defect site, and the local density at the bone defect site was lower than the surrounding bones in the blank group. In the control group, the bone density at the bone defect site was slightly lower than the surrounding bones, no obvious bone callus was observed, and a small amount of bone allograft residual was visible. In the experimental group, the bone density at the bone defect site was slightly lower than the surrounding bones, but the situation was better than in the blank group and worse than in the control group; bone callus formation was observed, and a small amount of bone allograft residual was visible. At 12 weeks, a small amount of bone callus formed around the bone defect site, and the density at the bone defect site decreased in the blank group. In the control group and the experimental group, bone density at the bone defect site was equivalent to the surrounding bones, and a shadow of bone allograft residual was visible (Figure 1).

Lane-Sandhu score

Lane-Sandhu scoring was performed on the bone defect sites of all the animals in all 3 groups. Homogeneity test of variance was performed on Lane-Sandhu scores at all postoperative time points in the blank, control, and experimental groups, and the results verified the homogeneity of variance of the scores ($P > 0.10$). Then, multiple sample averages were compared pairwise by SNK-t test. The results suggested that there were no statistically significant differences among the scores obtained from the blank, control, and experimental group in postoperative week 2 ($P > 0.05$). In postoperative weeks 4, 8, and 12, however, the average scores obtained from the experimental and control groups were higher than in the blank group ($P < 0.05$), but there was no statistically significant difference between the average scores in the experimental and control groups ($P > 0.05$) (Table 3, Figure 2).

Bone density detection

The bone densities at the bone defect sites in the animals from all 3 groups were measured and the results are shown

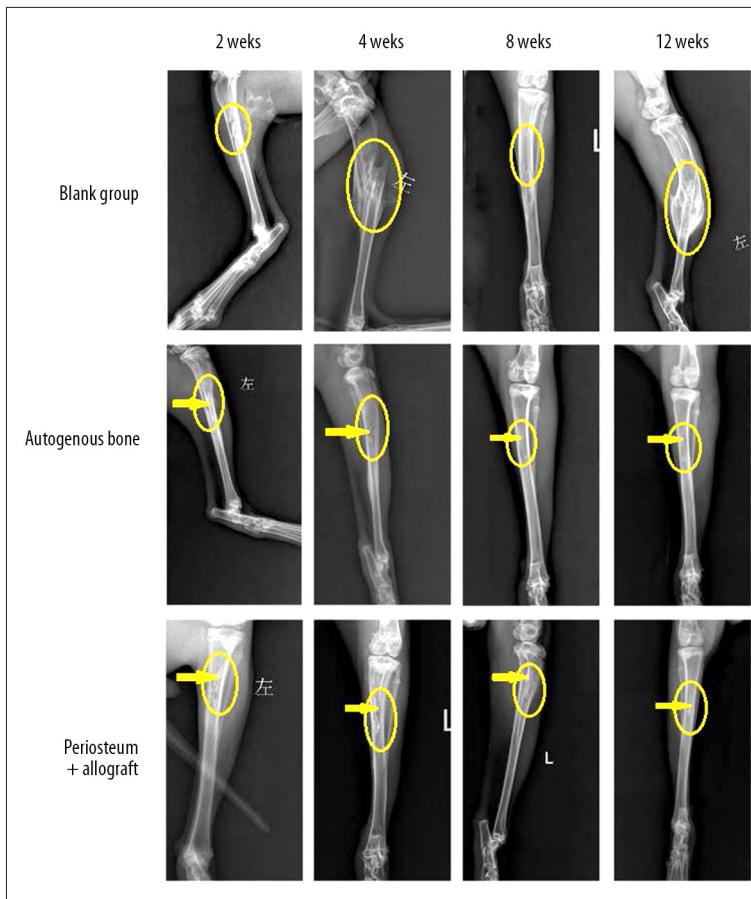


Figure 1. Imaging inspection results at different time points in the 3 groups, where the circled sites are bone defect regions and the sites pointed by arrows are shadows of residual bone allografts. At postoperative week 2, in the blank group, the defect can still be seen clearly, while in the autogenous group and combined therapy group, the bone allograft was visible, but the defect area started to become vague. At postoperative week 4 point, in the blank group, 1 animal had a refracture, but in the other 2 groups, no refracture can be seen, the bone density at the bone defect sites was lower than in surrounding bones, and shadows of bone allograft were visible. At postoperative week 8, in the blank group, the defect area can be seen clearly, with bone density lower than in the surrounding area, while in the autogenous group and combined therapy group, the bone density at the defect site was lower, but it was higher than the blank group, and shadows of bone allograft are visible. At postoperative week 12, in the blank group, 1 animal had a refracture and reunion, while in the autogenous group and combined therapy group, no animals had refracture, and the bone density at the defect site was equivalent to the density of the surrounding bones, and a small amount of bone allograft residual was visible.

in Table 4 and Figure 3. Homogeneity test of variance was performed on the bone density values at all postoperative time points in blank, control, and experimental groups, and the results verified the homogeneity of variance of the bone density values ($P > 0.10$). Then, multiple sample averages were compared pairwise by SNK-t test, and the results suggested that, in postoperative week 2, the bone density results obtained from the control group were higher than in the experimental ($P < 0.05$) and blank groups ($P < 0.05$). In postoperative weeks 4, 8, and 12, the averages obtained from the experimental and control group were higher than in the blank group ($P < 0.05$), but there were no statistically significant differences between the averages from the experimental and control groups ($P > 0.05$).

Tissue and histochemical examination

A large amount of erythrocyte diapedesis was observed in the blank group (Figure 4A) during the second week of the study. In that same time frame, a large amount of inflammatory cell infiltration and erythrocyte diapedesis was observed around the bone allograft in both the control group (Figure 4B) and experimental group (Figure 4C) in that time period. No obvious bone trabecula formation was observed in any of the groups.

During week 4 of the study (Figure 4D), the blank group showed increased inflammatory cell infiltration and a small amount of vasculogenesis occurred. In the control group (Figure 4E), inflammatory cell infiltration increased compared with before, and a large amount of vasculogenesis was observed; new bone trabeculas were visible at the distal-proximal joint of the bone defect region formed near the vessels. The joint site presented a gradual creeping substitution situation where the new bones and the sequestrums interwove together. In the experimental group (Figure 4F), inflammatory cell infiltration occurred around the bone allograft, but the infiltration amount was less than in the blank group, and new vessels and new bone trabeculas had formed.

During week 8, vasculogenesis was observed and the inflammatory cell infiltration and erythrocyte diapedesis decreased significantly in the blank group compared with before. In the control group (Figure 4G), new bone trabeculas were visible at the distal-proximal joint of the bone defect region. Compared with week 8, the new bone trabeculas were more ordered and

Table 3. Lane-Sandhu radiographic scoring results ($\bar{x}\pm s$).

Group	2 weeks	4 weeks	8 weeks	12 weeks
Blank group	0.52±0.12	0.63±0.23	1.64±0.94	2.36±0.74
Control group	0.61±0.11	3.97±0.17	6.16±0.34	8.76±0.64
Experiment group	0.58±0.18	3.33±0.67	5.73±0.77	7.93±0.57

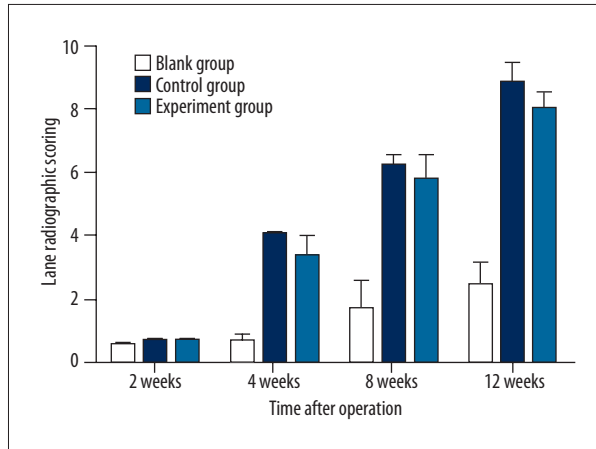


Figure 2. The Lane-Sandhu radiographic score of the three groups. There were no statistical difference among the three groups 2 weeks after the surgical procedure operation ($P>0.05$). In the time point of 4, 8, 12 weeks after the surgical procedure, the control group and the experiment group had a higher score than the blank group ($P<0.05$), but no statistical differences could be observed between the control and the experiment groups ($P>0.05$).

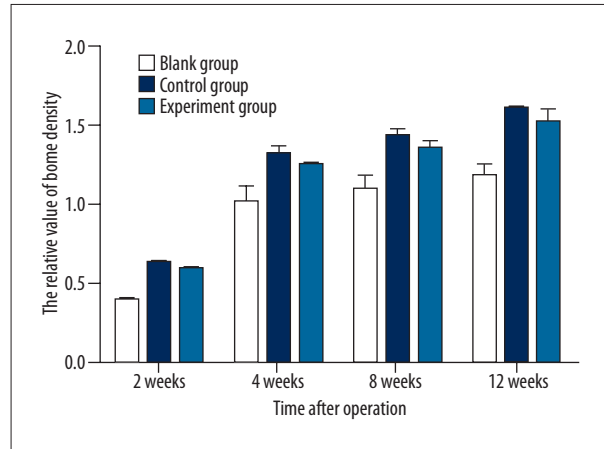


Figure 3. In postoperative week 2, the bone density results obtained from the control group were higher than in the experimental group ($P<0.05$) and in the blank group ($P<0.05$). In postoperative weeks 4, 8, and 12, the averages obtained from the experimental and control groups were higher than in the blank group ($P<0.05$), but there were no statistically significant difference between the averages from experimental and control groups ($P>0.05$).

Table 4. Relative value of bone density ($\bar{x}\pm s$) (g/cm^2).

Group	2 weeks	4 weeks	8 weeks	12 weeks
Blank group	0.398±0.019	1.002±0.104	1.087±0.083	1.169±0.067
Control group	0.638±0.024	1.301±0.054	1.419±0.039	1.593±0.028
Experiment group	0.593±0.018	1.239±0.029	1.337±0.051	1.508±0.072

there was no obvious erythrocyte diapedesis; inflammatory cell infiltration was as observed in the experimental group (Figure 4H). New bone trabeculas were found around the distal-proximal joint of the bone defect region; both the bone allograft and the joint presented a creeping substitution situation where the new bones and the sequestrums interwove together. Therefore, the arrangement was rather disordered and there still was a small amount of inflammatory cell infiltration.

During week 12 of the experiment, in the blank group, a small amount of inflammatory cell infiltration was still visible, and the inflammatory cells were found to embrace and decompose

the necrotic bones in the blank group. In the control group, the new bone trabeculas were ordered and there was no obvious inflammatory cell infiltration or erythrocyte diapedesis. In the experimental group, the new bone trabeculas were ordered, but there still was a little bone allograft residual (Figure 4I) and the bone allograft was embraced by the inflammatory cells.

Fluorescence quantitative PCR detection

The result of SPP-1 test (Figure 5) suggested that SPP-1 gene expression in the experimental group was higher than in the control group ($P<0.05$) in postoperative weeks 2, 4, and 8. The

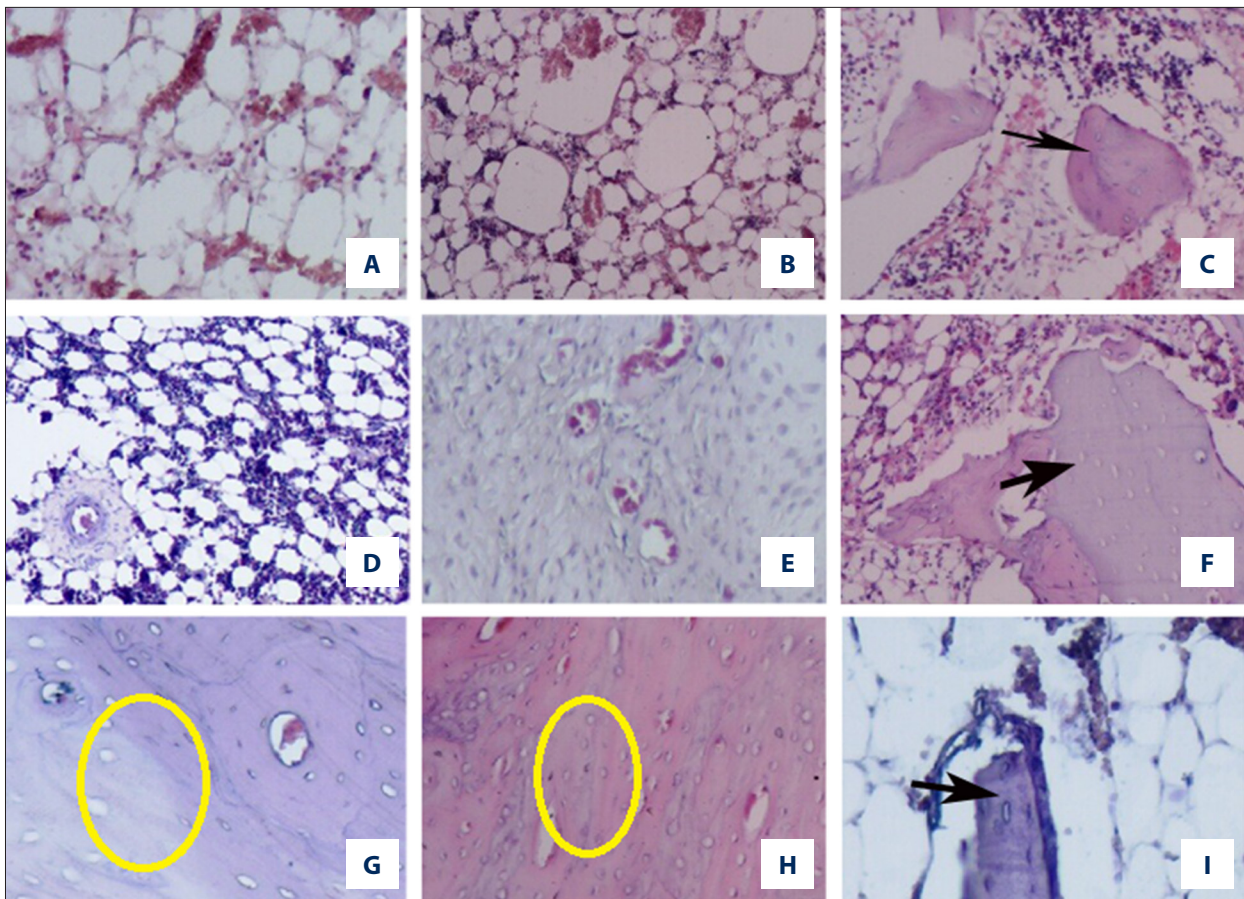


Figure 4. HE staining results at all time points in the 3 groups: the region pointed to by the arrow is necrotic bone allograft. (A) large amount of erythrocyte diapedesis occurred in week 2 in the blank group (200× magnification); (B, C) a small amount of erythrocyte diapedesis and a considerable amount of inflammatory cell infiltration were observed in week 2 in the control group and experimental group (200× magnification); (D) a large amount of inflammatory cell infiltration and a small amount of vasculogenesis took place in week 4 in the control group (200× magnification); (E) during week 4 in the control group, the new bone trabeculas were disordered and many new vessels formed (200× magnification); (F) inflammatory cells wrapped the necrotic bone allograft in week 4 in the experimental group (200× magnification); (G) the new bone trabeculas were more ordered in week 8 than before in the control group (200× magnification); (H) during week 8 in the experimental group, the grafting site presented a creeping substitution situation where the new bones and the sequestrums interwove together, so the arrangement was rather disordered (200× magnification); (I) the residual bone allograft was wrapped by the inflammatory cells in week 12 in the control group (400× magnification). Picture Caption: the site pointed to by the arrow is bone allograft and the circled site is the creeping substitution region where new bones and sequestrums interwove together.

difference in expression was highest in postoperative week 4 ($P < 0.01$). The result of BMP-2 test suggested that the BMP-2 gene expression in the experimental group was higher than in the control group ($P < 0.01$) in postoperative weeks 2 and 4. The result of Col $\alpha 1$ test suggested that the gene expression in the control group was higher than in the experimental group ($P < 0.05$) in postoperative weeks 2, 4, 8, and 12. The expression in postoperative weeks 2 and 12 was significantly higher in the control group than in the experimental group ($P < 0.01$). The result of the VEGF test suggested that VEGF gene expression in the experimental group was higher than in the control group ($P < 0.05$) in postoperative weeks 2 and 4. The difference in expression was highest in postoperative week

4 ($P < 0.01$). The aforementioned results demonstrated that in the bone defect repair therapy by periosteum combined with bone allograft, the repair effect is conducted through increases in SPP-1, BMP-2, and VEGF gene expression. In autogenous bone therapy, the repair effect is conducted through the increase in Col $\alpha 1$ gene expression.

Discussion

In studies of bone defects, the establishment of a bone defect model is crucial to the success of the experiments. An appropriate bone defect model should be selected according

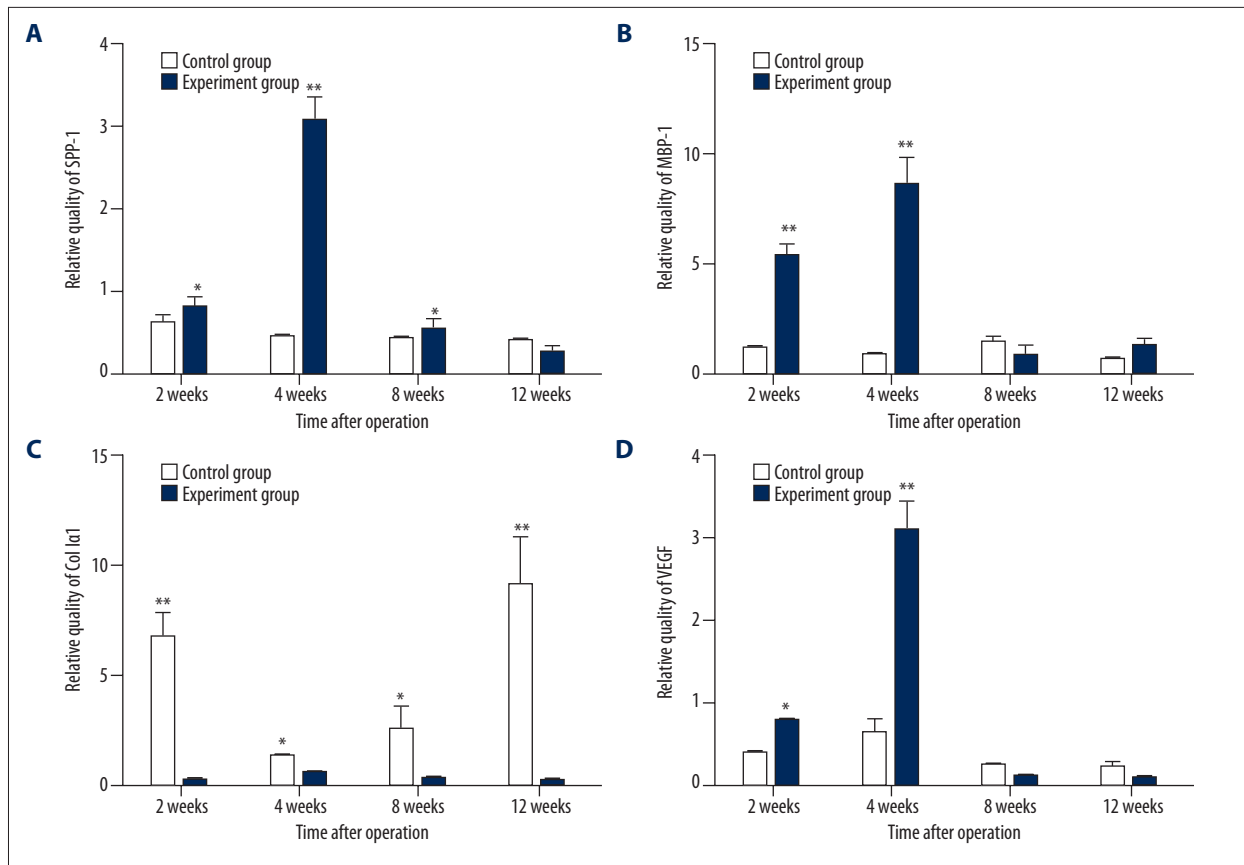


Figure 5. Fluorogenic quantitative PCR results of SPP-1, BMP-2, Col α 1, and VEGF expression in the control and experimental groups. (A) is the SPP-1 expression, the results suggested that the SPP-1 gene expression in the experimental group was higher than in the control group (* $P < 0.05$) in postoperative weeks 2, 4, and 8; the difference in expression was highest in postoperative week 4 (** $P < 0.01$). (B) is the BMP-2 expression. The results suggest that the BMP-2 gene expression in the experimental group was higher than in the control group (** $P < 0.01$) in postoperative weeks 2 and week 4. (C) is the Col α 1 expression, which suggests that Col α 1 gene expression in the control group was higher than in the experimental group (* $P < 0.05$) in postoperative weeks 2, 4, 8, and 12. The expression in postoperative weeks 2 and 12 was significantly higher in the control group than in the experimental group (** $P < 0.01$). (D) is the VEGF expression. The result suggests that VEGF gene expression in the experimental group was higher than in the control group (* $P < 0.05$) in postoperative week 2 and 4. The difference in expression was highest in postoperative week 4 (** $P < 0.01$).

the objective of the study. So far, there have been many animal models reported. Rabbits are used frequently in orthopedic experiments, especially in treatment efficacy studies, because rabbit bones have bone defect characteristics similar to the biomechanical performance of human bones [20]. Pazzaglia et al. conducted an experiment with New Zealand white rabbits and found that hind limbs have a Haversian system, able to bear more weight [21], which is similar to the lower limbs of humans. An earlier study indicated that an 8-mm diameter round bone defect in the tibia meets the requirement of an experimental animal model of bone defect [18]; this model can be used in biocompatibility, osteoinduction capability, and osteogenic capability studies on bone-substitute materials. It does not need external fixation, reducing the factors affecting the bone defect healing and thus lowering the risk of secondary fracture. It provides an important animal model for

the development of bone-substitute stent materials and how bone defects repair themselves.

The efficacy showed in this study was objectively assessed by the Lane-Sandhu scoring system [19] by 3 independent examiners familiar with the scoring criteria. The results suggested that there were no statistically significant differences at the 4 postoperative time points between the experimental group (bone defect treated by periosteum combined with bone allograft) and the criterion standard group (bone defect treated by autogenous bone graft). The bone density at the bone defect sites also was evaluated, and the results also suggested that the combined therapy of periosteum and bone allograft could recover the bone density at the defect sites. Therefore, we proved that the combined therapy of periosteum and bone allograft could attain similar efficacy to autogenous

bone grafting in treating bone defects and could be taken as an optional therapy when autogenous bone is not sufficient.

Imaging inspections and HE staining results showed part of the mechanisms of periosteum repair of bone defect. In postoperative week 2 in the simple periosteum wrapping group, erythrocytes accounted for most infiltrates, which was consistent with the infiltrate condition after normal fractures. In postoperative week 2 in the simple autogenous bone grafting group and the periosteum and bone allograft combined therapy group, inflammatory cells accounted for most infiltrates. Combined with the fact that imaging inspections showed that the bone allograft still existed, inflammatory cell infiltration was considered to be related to the bone allograft. This could be explained by the manifestations of the control group in postoperative week 12. In postoperative week 12, a small amount of bone allograft residual was still visible by the imaging inspection in the control group, so the HE staining result showed that inflammatory cells were still infiltrating and wrapping the bone allograft. With regard to the therapeutic mechanism, the repair in the blank group (bone defect group) is conducted through the formation of bone calluses, so different extents of bone callus formations were found in all animal groups. In the blank group at postoperative time points, and in the control group and experimental group, the filling is performed on the bone allograft, so no obvious bone callus formation was observed at the defect area.

The healing mechanisms of the experimental and control groups were quite different, however. This was shown by the relevant gene expression situation: in our study, we found that the expression of SPP-1, BMP-2, and VEGF in the experimental group was higher than in the control group, especially in postoperative weeks 2 and 4 ($P < 0.05$). These genes probably participated in the therapeutic process of bone allograft combined with periosteum, but in the autogenous bone graft therapy, the main repair mechanism was to increase the expression of Col $\alpha 1$ ($P < 0.05$).

What is the reason for such results?

SPP-1 is the gene sequence of osteopontin (OPN), which plays an important role in the mineralization and absorption process

References:

1. VandeVord PJ, Nasser S, Wooley PH: Immunological responses to bone soluble proteins in recipients of bone allografts. *J Orthop Res*, 2005; 23(5): 1059–64
2. Hofmann A, Konrad L, Hessmann MH et al: The influence of bone allograft processing on osteoblast attachment and function. *J Orthop Res*, 2005; 23(4): 846–54
3. Mourikis A, Mankin HJ, Hornicek FJ et al: Treatment of proximal humeral chondrosarcoma with resection and allograft. *J Shoulder Elbow Surg*, 2007; 16(5): 519–24
4. Zoubos AB, Triantafyllopoulos IK, Babis GC et al: A modified matti-russe technique for the treatment of scaphoid waist non-union and pseudarthrosis. *Med Sci Monit*, 2011; 17(2): MT7–12
5. Xie XT, Gao YS, Zhang CQ: Salvage of a femoral nonunion after primary non-Hodgkin's lymphoma of bone: A case report and literature review. *Med Sci Monit*, 2011; 17(11): CS138–43
6. Maculé F, Segur JM, Vilalta C, Suso S: The use of fascia lata and bone allograft for uncontained defects in revision knee arthroplasty. *Ann Transplant*, 2004; 9(3): 72–73

of bone matrix [22]. Its major effect is to regulate the balance of bone metabolism. Although it plays a crucial role in the activation of osteoclasts [23–27], the expression of SPP-1 is affected by various growth factors and differentiation factors, such as BMP-2 and VEGF [28]. In postoperative weeks 2 and 4, the gene expression of BMP-2 and VEGF in the experimental group was higher than in the control group, and this probably affected the expression of SPP-1, leading to the increase in OPN expression, thus the SPP-1 expression was higher in control group in week 2, 4, and 8. The reason for the elevations in BMP-2 and VEGF expression was probably that the active protein factors were destroyed during the production process of bone allograft, but the activity of protein factors was not affected during the production process of autogenous bone. This was further evidenced by the fact that collagen I (Col $\alpha 1$) expression was lower in the experimental group than in the control group. A total of 80% of collagens are expressed in bones, keeping the integrity of bone tissue, so the bone allograft contains a large amount of Col $\alpha 1$ proteins, thus impacting the protein production.

Conclusions

The aim of this study was to observe the efficacy and mechanism of the combined therapy of periosteum and bone allograft in critically-sized defect models in New Zealand white rabbits. The results of the study suggest that the efficacies of the combined therapy (periosteum combined with bone allograft) and the criterion standard therapy (autogenous bone grafting) are equivalent in treating bone defects. The mechanisms of the 2 therapies, however, probably were different. The mechanism of combined therapy of periosteum and bone allograft may involve the increase in the expression of OPN, BMP-2, and VEGF, while the autogenous bone graft therapy may be related to the increase in the expression of Col $\alpha 1$. Additional study of these effects is needed.

Statement

This experiment is supported by Guangdong Natural Science Foundation (S2011010001347). The funders had no role in study design, data collection and analysis, decision to publish, or preparation of the manuscript.

7. Abe Y, Takahata M, Ito M et al: Enhancement of graft bone healing by intermittent administration of human parathyroid hormone (1-34) in a rat spinal arthrodesis model. *Bone*, 2007; 41(5): 775-85
8. Bassett C: Current concepts of bone formation. *J Bone Joint Surg Am*, 1962; 44(6): 1217
9. Macewen W, Peltier L F: The Classic: The growth of bone chapter III. Osteogenic power of bone bereft of periosteum. *Clin Orthop Relat Res*, 1983; 174: 5-14
10. Knize DM: The influence of periosteum and calcitonin on only bone graft survival a roentgenographic study. *Plast Reconstr Surg*, 1974; 53(2): 190-99
11. Buser D, Dula K, Belsler U et al: Localized ridge augmentation using guided bone regeneration: 1 Surgical procedure in the maxilla. *Int J Periodontics Restorative Dent*, 1993; 13(1): 29-45
12. Zhang X, Xie C, Lin A et al: Periosteal progenitor cell fate in segmental cortical bone graft transplantations: implications for functional tissue engineering. *J Bone Miner Res*, 2005; 20(12): 2124-37
13. Poussa M, Rubak J, Ritsila V: The effect of the thickness of the cortical bone on bone formation by osteoperiosteal grafts. A comparative study employing routine histological stains and triple fluorochrome labelling. *Acta Orthop Scand*, 1980; 51(1): 29-35
14. Berggren A, Weiland AJ, Ostrup LT et al: Microvascular free bone transfer with revascularization of the medullary and periosteal circulation or the periosteal circulation alone. A comparative experimental study. *J Bone Joint Surg Am*, 1982; 64(1): 73-87
15. Enneking WF, Campanacci DA: Retrieved human allografts: a clinicopathological study. *J Bone Joint Surg Am*, 2001; 83(7): 971-86
16. Fox EJ, Hau MA, Gebhardt MC et al: Long-term followup of proximal femoral allografts. *Clin Orthop Relat Res*, 2002; 397: 106-13
17. DePaula CA, Truncale KG, Gertzman AA et al: Effects of hydrogen peroxide cleaning procedures on bone graft osteoinductivity and mechanical properties. *Cell Tissue Bank*, 2005; 6(24): 287-98
18. de Girolamo L, Arrigoni E, Stanco D et al: Role of autologous rabbit adipose derived stem cells in the early phases of the repairing process of critical bone defects. *J Orthop Res*, 2011; 29(1): 100-8
19. Lane JM, Sandhu HS: Current approaches to experimental bone grafting. *Orthop Clin North Am*, 1982; 18(2): 213-25
20. Mapara M, Thomas BS, Bhat KM: Rabbit as an animal model for experimental research. *Dental Res J*, 2012; 9(1): 111-18
21. Pazzaglia UE, Zarattin G, Giacomini D et al: Morphometric analysis of the canal system of cortical bone: an experimental study in the rabbit femur carried out with standard histology and micro-CT. *Anat Histol Embryol*, 2010; 39(1): 17-26
22. Reinholt FP, Hultenby K, Oldberg A et al: Osteopontin – a possible anchor of osteoclasts to bone. *Proc Natl Acad Sci USA*, 1990; 87(12): 4473-75
23. Mark MP, Prince CW, Oosawa T et al: Immunohistochemical demonstration of a 44-kD phosphoprotein in developing rat bones. *Histochem Cytochem*, 1987; 35(7): 707-15
24. Owen TA, Aronow M, Shalhoub V et al: Progressive development of the osteoblast type *in vitro*: Reciprocal relationships in expression of genes associated osteoblast proliferation and differentiation during formation of the bone extracellular matrix. *Cell Physiol*, 1990; 143(3): 420-30
25. Oldberg A, Franzen A, Heinegard D: Cloning and sequence analysis of rat bone sialoprotein (osteopontin) cDNA reveals an Arg-Gly-Asp-Asp binding sequence. *Prog Natl Acad Sci USA*, 1986; 83(23): 8819-23
26. Somerman MJ, Prince CW, Sauk JJ et al: Mechanism of fibroblast attachment to bone extracellular matrix: role of a 44 kilo delton bone phosphoprotein. *Bone Miner Res*, 1987; 2(3): 259-65
27. Hunter GK, Goldberg HA: Modulation of crystal format ion by bone phosphoproteins: role of glutamic acidrich sequences In the nucleation of hydroxyapatite by bone sialoprotein. *Biochem*, 1994, 302(Pt 1): 175-79
28. Chatterjee M: Vitamin D and genomic stability. *Mutat Res*, 2001; 475(1-2): 69-87